Localization of electrons in a one-dimensional conductor with strong disorder

A. A. Gogolin

L. D. Landau Institute of Theoretical Physics, USSR Academy of Sciences
(Submitted 14 December 1978)
Zh. Eksp. Teor. Fiz. **76**, 1759–1774 (May 1979)

The localization of electronic states in a one-dimensional conductor with a strong random potential is investigated. Multiple scattering of an electron by an individual impurity is taken into account within the framework of Berezinskiĭ's diagram method. The dependence of the localization length on the value of the impurity potential is obtained. The frequency dependences of the conductivity and of the dielectric constant are calculated.

PACS numbers: 72.15.Nj, 71.55.Jv

1. INTRODUCTION

Much interest is being paid at present to Mott localization of electrons in one-dimensional disordered conductors. The study of this phenomenon is particularly important in connection with the experimental research on quasi-one-dimensional organic conductors based on the TCNQ molecule. Electron localization means that the ordinary static conduction and electrons diffusion do not take place in such conductors. The localization phenomenon was qualitatively predicted by Mott and Twose,[1] and was later quantitatively investigated in a number of studies.[2] A direct calculation of the low-frequency asymptotic form of the conductivity $\mathrm{Re}\sigma(\omega)$ as $\omega \to 0$ ($\mathrm{Re}\sigma(\omega) \propto \omega^2 \ln^2 \omega$) was first made by Berezinskii.[3] He developed a diagram technique and derived equations which made it possible subsequently to calculate the density distribution of the localized electronic state[4] and the frequency dependence of the conductivity at arbitrary ω.[5] Another method of calculating the conductivity was proposed by Abrikosov and Ryzhkin.[6] Berezinskiĭ's diagram method was used to solve the problem of calculating the conductivity that appears when the electron-phonon interaction is taken into account.[7] It was shown subsequently that this mechanism can explain the characteristic temperature dependence of the conductivity and of the dielectric constant in TCNQ salts with asymmetric cations.[8]

In all the cited studies they considered localization in a weak random potential. It was assumed that the potential $u(x)$ of an individual impurity satisfies the Born condition

$$\alpha = \frac{1}{v_F}\int_{-\infty}^{\infty} u(x)\,dx \ll 1.$$

The present paper is devoted to an investigation of the one-dimensional localization of the electrons in a random potential of arbitrary size. This problem is of interest because in real quasi-one-dimensional conductors with strong structural disorder, $Qn(TCNQ)_2$ and $Adz(TCNQ)_2$, the Born condition $\alpha \ll 1$ is violated, viz., in these substances $\alpha \sim 1$ (Ref. 8).

2. SELECTION OF DIAGRAMS AND DERIVATION OF FUNDAMENTAL EQUATIONS

We consider a one-dimensional system of noninteracting electrons with a dispersion law $\varepsilon(p)$, situated in a random potential $V(x)$. We assume that the random potential $V(x)$ is produced by randomly disposed impurities with a potential $u(x)$:

$$V(x) = \sum_j u(x - a_j), \tag{1}$$

a_j are the coordinates of the impurities.

To determine the character of the localization, of the electric conductivity, and of the dielectric constant, it is necessary to calculate the correlation functions of the density and current operators $j^0(x)$ and $j^1(x)$. A diagram technique convenient for this purpose was developed in Refs. 3 and 7.

We consider the case of an arbitrary, i.e., not small, potential $u(x)$. Therefore not only the paired correlators, but also all other correlators of the impurity potential $U_n(x_1, \ldots, x_n)$, $n = 1, 2; \ldots$ differ from zero when averaged over the impurity positions. The averaging over the position of the impurities a_j will be carried out in accord with the usual "cross" technique,[9] i.e., by integrating with respect to a_j and multiplying by L^{-N}, where L is the dimension of the system and N is the total number of impurities. It is easily seen that in this case the correlator $U_n(x_1, \ldots, x_n)$ takes the form

$$U_n(x_1, \ldots, x_n) = c\int_{-\infty}^{\infty} da \prod_{i=1}^{n} u(x_i - a), \tag{2}$$

where c is the impurity concentration.

On the diagrams, the correlator U_n is represented by wavy lines emerging from the point a and terminating at the points x_i. One of the simplest diagrams of this type is shown in Fig. 1a. All the diagrams are drawn in the coordinate-energy representation and are already ordered with respect to x. We assume that the impurity concentration c is small, and therefore the average distance c^{-1} between the impurities is large compared with the characteristic dimension b of the impurity potential and with the electron wavelength λ. The characteristic scale of integration with respect to a is the average distance c^{-1} between impurities. Since the integration with respect to x_i is over the region $|x_i - a| \sim b$, we can neglect, to the extent that $bc \ll 1$ is small, the diagrams of the type of Fig. 2, in which the integrations with respect to a and a' land in one and the same region of

 0038-5646/79/050895-08$02.40

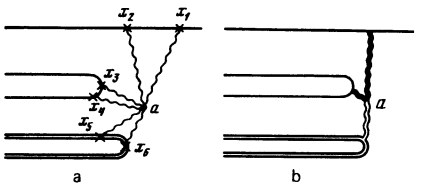

FIG. 1. Effective diagram for impurity vertex.

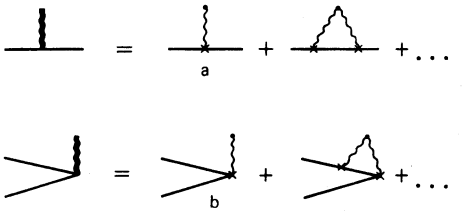

FIG. 3.

width b.

It is convenient to sum the diagrams in two steps. It is first necessary to sum over all the crosses that are involved in a single scattering act (see Fig. 3). The summation reduces to a replacement of the Born amplitude by the total one in a single scattering act and causes the diagram of Fig. 1a to go over into the effective diagram of Fig. 1b. All the crosses then land in the point a (since the integrations with respect to x_i have already been made), and the thick wavy lines correspond to the total amplitudes f_+ and f_- or forward and backward scattering. The thick wave line of Fig. 3a corresponds to the amplitude f_+, and the thick wave line of Fig. 3b corresponds to f_-. The double wavy lines differ from the solid ones by complex conjugation. For convience, the amplitudes f_+ and f_- include the factors $\mp i/v(\varepsilon)$, which occur when the zeroth Green's fuctions are factored out[7] ($v(\varepsilon)=d\varepsilon/dp$ is the velocity of an electron of energy ε). The amplitudes f_+ and f_- are connected by unitarity relations that take in the one-dimensional case, when account is taken of the additional factor i/v, the form[10]

$$-(f_+ + f_+^*) = |f_+|^2 + |f_-|^2, \tag{3}$$

$$-(f_- + f_-^*) = f_+ f_-^* + f_- f_+^*. \tag{4}$$

The backward scattering amplitude f_- is connected in the usual manner with the coefficient γ of reflection an individual impurity:

$$\gamma = |f_-|^2, \quad 0 \leqslant \gamma \leqslant 1 . \tag{5}$$

The quantity γ determines the electron mean free path $l = 1/c\gamma$. In the particular case of a δ-function impurity potential, $u(x) = u_0\delta(x)$, the amplitudes f_+ and f_- are simply expressed in terms of the potential:

$$f_+ = f_- = i\alpha/(1-i\alpha), \quad \alpha = u_0/v. \tag{6}$$

We shall not need the explicit expressions for f_+ and f_-, since all the results can be expressed in terms of γ.

The physical meaning of the effective diagram of Fig. 1b is that it is necessary to take into account, in one-dimensional problems, the multiple scattering of the electron by an individual impurity. Each individual scattering takes place with a total amplitude corresponding to the thick wavy lines, and the binding of the lines in a bundle means that all the acts of multiple scattering take place on one and the same impurity.

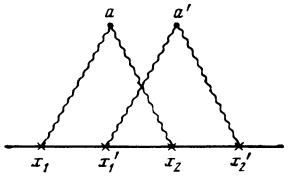

FIG. 2.

To calculate the correlation functions of the density operators and of the current we shall use the previously developed procedure.[3,7] Each diagram for the polarization loop, in the vertices of which stand the density or current operators, is divided into three parts that lie respectively to the left, in between, and to the right of the entry vertices x' and x. As will be shown below, the number of pairs of single and double lines in any section is the same. We designate these numbers in the sections x and x' by m and m'.

In the selection of the diagram we use the small parameter $(p_F l)^{-1} \sim \lambda c \ll 1$. This means that we neglect diagrams that contain rapildy oscillating factors of the type $\exp(ip_F a_j)$, and retain diagrams containing only slowly varying factors of the type $\exp(i\omega a_j/v)$, where ω is the low frequency of the external field. It is easily seen that by inserting into the section of the diagram a bundle of wavy lines such as in Fig. 1b, which changes the number of pairs of single lines in the section by an amount s_1 and the number of pairs of double lines by s_2, we add to the diagram a factor $\exp\{2ia(s_2 p(\varepsilon) - s_1 p(\varepsilon+\omega))\}$. The rapidly oscillating factors of the type $\exp(ip_F a)$ cancel out only if $s_1 = s_2 = s$. Therefore the numbers of pairs of single and double lines change only in symmetrical fashion and are always equal to one another.

Denoting by $R_m(x)$ the part of the polarization loop that lies to the right of the input vertex x, and considering the passage of individual bundles of wavy lines through the section x as the latter is displaced, we can easily obtain equations for $R_m(x)$. The diagram-technique derivation of these equations is illustrated in Fig. 4. It is easily seen that a change of the number of pairs of single lines in the section by an amount s is effected decreasing it by k (this can be done in C_m^k ways, by inserting total angle vertices of the type of Fig. 3b), and increasing it by $k+s$ (this can be done in $C_{m+s}^{k+s}{}_{-1}$ ways, by inserting the corresponding spatially inverted angle

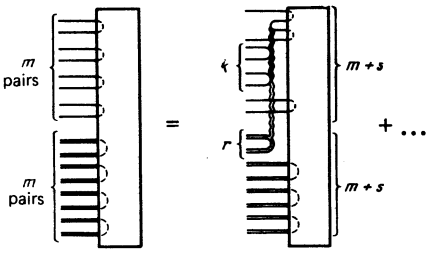

FIG. 4. Scheme for the construction of the equations for R_m.

vertices). The change of the number of pairs of lines in the section is effected only by rotary vertices of the type of Fig. 3b. Nonrotary vertices such as Fig. 3a can be inserted in the diagram of Fig. 4 in arbitrary amounts n, starting with $n=0$ all the way to $n=2m-2k$, but they must not land on lines already touched by rotary vertices. This can be done in C_{2m-2k}^{n} ways. Summation over the number of nonrotary vertices and over all the manners of their arrangement leads to the appearance of the factors $(1+f_+)^{2m-2k}$ and $(1+f_+^*)^{2m-2r}$. in the equation. The equations for the right-hand sides of $R_m(x)$ take ultimately the form

$$-\frac{d}{dx}R_m=c\sum_s V_{ms}R_{m+s}e^{-2is\omega x/v}-cR_m-cR_0|f_-|^{2m}e^{2im\omega x/v},$$

$$V_{ms}=\sum_{k,r}C_m^k C_{m+s-1}^{k+s}(f_-)^{2k+s}(1+f_+)^{2m-2k}C_m^r C_{m+s-1}^{r+s}(f_-^*)^{2r+s}(1+f_+^*)^{2m-2r}. \quad (7)$$

The appearance of the second term is connected with the need for eliminating from the sum the term with $k=r=s=0$, and the third term corresponds to $s=-m$ and $k=r=m$. The equation for the central parts $Z_{m'm}(x', x)$ are similar in form:

$$\frac{d}{dx}Z_{m'm}=c\sum_s W_{ms}Z_{m'm+s}e^{2is\omega x/v}-cZ_{m'm}+\frac{i\omega}{v}Z_{m'm}, \quad (8)$$

$$W_{ms}=\sum_{k,r}C_m^k C_{m+s}^{k+s}(f_-)^{2k+s}(1+f_+)^{2m-2k+t}C_m^r C_{m+s}^{r+s}(f_-^*)^{2r+s}(1+f_+^*)^{2m-2r+t}.$$

To simplify Eqs. (7) and (8) we use the unitarity conditions (3) and (4). From (3) and (4) it follows that

$$|1+f_+|^2=1-\gamma, \quad (9)$$

$$f_-(1+f_+^*)=-f_-^*(1+f_+). \quad (10)$$

Substituting (9), (10), and (5) in (7) and (8) we get

$$(f_-)^{2k+s}(1+f_+)^{2m-2k}(f_-^*)^{2r+s}(1+f_+^*)^{2m-2r}=(-1)^{k+r}\gamma^{k+r+s}(1-\gamma)^{2m-k-r}. \quad (11)$$

The substitution $R_m(x)=e^{2im\omega x/v}R_m$ reduces (7) to the form

$$-ivmR_m=\frac{1}{\gamma}\sum_s V_{ms}R_{m+s}-\frac{1}{\gamma}R_m+R_0\gamma^{m-1}, \quad m=1;\ 2;\ \ldots$$

$$V_{ms}=\sum_{k,r}C_m^k C_{m+s-1}^{k+s}C_m^r C_{m+s-1}^{r+s}(-1)^{k+r}\gamma^{k+r+s}(1-\gamma)^{2m-k-r}. \quad (12)$$

Here $\nu=2\omega l/v=2\omega\tau$, and $R_0=1$. The density and current correlators X^0 and X^1 are expressed in terms of the quantities R_m and $Z_{m'm}$ with the aid of the usual relations[3,7]

$$X^a(\omega, k)=\frac{2l}{v}\left[\frac{v}{2}\right]^{2a}\sum_{m=0}^{\infty}P_m^a(\omega)[Q_m^a(\omega, k)+Q_m^a(\omega, -k)], \quad (13)$$

$$P_m^0=1/2(R_m+R_{m+1}), \quad (14)$$

$$P_m^1=R_m-R_{m+1}, \quad (15)$$

$$Q_m^a(\omega, k)=\frac{1}{l}\sum_{m'=0}^{\infty}\int_{x'}^{\infty}dx e^{ik(x'-x)-2i\omega m'x'/v}Z_{m'm}(x', x)e^{2i\omega mx/v}P_{m'}^a. \quad (16)$$

The quantities $Q_m^a(\omega, k)$ satisfy the difference equation

$$-iv\left(m+\frac{1}{2}\right)Q_m^a=\frac{1}{\gamma}\sum_s W_{ms}Q_{m+s}^a-\frac{1}{\gamma}Q_m^a-i\varkappa Q_m^a+P_m^a,$$

$$W_{ms}=\sum_{k,r}C_m^k C_{m+s}^{k+s}C_m^r C_{m+s}^{r+s}(-1)^{k+r}\gamma^{k+r+s}(1-\gamma)^{2m-k-r+t}. \quad (17)$$

Here $\varkappa=kl$.

We note in connection with the derivation of Eqs. (12) and (17) that in one-dimensional systems, in contrast to three-dimensional ones, allowance for the strong interaction with the impurities at low concentration of the latter does not reduce to a simple replacement of the Born amplitude α by the total amplitude f. The reason is that in a one-dimensional system, owing to the strong interference of the electron waves, the individual scattering acts are not independent. Therefore even at a low impurity concentration, localization causes multiple scattering of an electron by one impurity and the interference of the corresponding waves to become important. These processes, which are described by diagrams of the type of Fig. 1, lead to a substantial dependence of all the quantities on the parameter γ.

3. LOCALIZATION OF ELECTRONS

To solve the question of electron localization it is necessary to calculate the static conductivity

$$\sigma(0)=\lim_{\omega\to 0}\sigma(\omega)$$

and the asymptotic form of the density correlator as $t\to\infty$. The conductivity $\sigma(\omega)$ is determined in accord with the Kubo formula by the current correlator X^1:

$$\sigma(\omega)=\sigma_0\sum_{m=0}^{\infty}P_m^1Q_m^1, \quad (18)$$

$$\sigma_0=2e^2l/\pi S, \quad (19)$$

where S is the cross section area per conducting filament.

It will be shown later that all the electronic states in the system are localized and $\sigma(0)=0$. To prove this fact it is necessary to investigate the structure of Eqs. (12) and (17) as $\omega\to 0$. We consider first the case of small $\gamma\ll 1$. Discarding the terms of higher order in γ, we obtain from (12) and (17) the Berezinskii equations[3]:

$$-ivmR_m=m^2(R_{m-1}+R_{m+1}-2R_m), \quad (20)$$

$$-iv\left(m+\frac{1}{2}\right)Q_m^a=(m+1)^2(Q_{m+1}^a-Q_m^a)-m^2(Q_m^a-Q_{m-1}^a)-i\varkappa Q_m^a+P_m^a. \quad (21)$$

From the form of Eqs. (20) and (21) it follows that at small $\nu\ll 1$ the major contribution in the sums (18) over $m\sim\nu^{-1}\gg 1$. At large m we can go over in (20) and (21) from the discrete variable m to the continuous one $p=-ivm$, and go in (18) from summation over m to integration with respect to p.

Changing in (18), (20), and (21) to the variable p, we obtain with allowance for the definition (15)

$$\sigma(\nu)=(-iv)\sigma_0\int_0^{\infty}dp\frac{dR}{dp}q^1(p)+O(\nu^2), \quad (22)$$

where the functions $R(p)$ and $q^1(p)$ satisfy differential equations that do not contain the frequencies ν:

$$pR=p^2\,d^2R/dp^2, \quad (23)$$

$$pq^1=p^2\frac{d^2q^1}{dp^2}+2p\frac{dq^1}{dp}+\frac{dR}{dp}. \quad (24)$$

It follows from (22) that $\sigma(0)=0$ at $\gamma\ll 1$. To prove this in the general case of arbitrary γ, we consider

Eqs. (12) and (17) at large $m \sim \nu^{-1}$. We begin with (12). It will be shown later that in the sums over s in (12) the important role is played by small $s \sim 1 \ll m$. Therefore R_{m+s} can be represented in the form

$$R_{m+s} = \sum_{v=0}^{\infty} \frac{s^v}{v!} \left(\frac{d}{dm}\right)^v R_m. \tag{25}$$

Substituting in (12)

$$(1-\gamma)^{2m-k-r} = \sum_d C_{2m-k-r}^d (-\gamma)^d,$$

introducing the new variable $n = k + r + s + d$, and representing s^v in the form $(\alpha d/d\alpha)^v \alpha^s|_{\alpha=1}$ we obtain the following equation for R_m at $m \gg 1$:

$$\begin{aligned} -i\nu m R_m &= \frac{1}{\gamma} \sum_{v=0}^{\infty} \frac{1}{v!} V_v(m) \left(\frac{d}{dm}\right)^v R_m - \frac{1}{\gamma} R_m + \gamma^{m-1}, \\ V_v(m) &= \sum_{n,k,r,d} \left(a \frac{d}{da} \right)^r \Big|_{a=1} \gamma^n (-1)^{k+r+d} C_{2m-k-r}^d C_m^k C_{m+n-k-r-d-1}^{n-r-d} \\ &\quad \times C_m^r C_{m+n-k-r-d-1}^{n-k-d} a^{n-k-r-d}. \end{aligned} \tag{26}$$

We represent the binominal coefficients $C_{m+n-k-r-d-1}^{n-r-d}$ and $C_{m+n-k-r-d-1}^{n-k-d}$ in the form

$$C_{m+n-k-r-d-1}^{n-r-d} = \frac{1}{2\pi i} \oint \frac{dx}{x^{n-r-d+1}(1-x)^{m-k}}, \tag{27}$$

$$C_{m+n-k-r-d-1}^{n-k-d} = \frac{1}{2\pi i} \oint \frac{dy}{y^{n-k-d+1}(1-y)^{m-r}}. \tag{28}$$

Integration with respect to x and with respect to y in (27) and (28) is along small circles of radius $\rho < 1$ around zero.

Substituting (27), (28), in (26) and first summing over d and next over k and over r, we get

$$\begin{aligned} -i\nu m R_m &= \frac{1}{\gamma} \sum_{n,r=1}^{\infty} \frac{1}{v!} \left(a \frac{d}{da}\right)^r \Big|_{a=1} \\ &\times \gamma^n \int \frac{dx\,dy}{(xy)^{n+1}} a^n \left[\frac{(a-x)(a-y)}{a^2(1-x)(1-y)}\right]^m \left(\frac{d}{dm}\right)^r R_m. \end{aligned} \tag{29}$$

We note that the use of the representation (27) and (28) enables us to include in the sum, in natural fashion, all the terms in (26).

It is easily seen that in the principal approximation of large m we have

$$\begin{aligned} \left(a \frac{d}{da}\right)^r \Big|_{a=1} \frac{1}{(2\pi i)^2} \int \frac{dx\,dy}{(xy)^{n+1}} a^n \left[\frac{(a-x)(a-y)}{a^2(1-x)(1-y)}\right]^m \\ \approx \frac{m^r}{(2\pi i)^2} \int \frac{dx\,dy}{(xy)^{n+1}} \left(\frac{x}{1-x} + \frac{y}{1-y}\right)^r. \end{aligned} \tag{30}$$

It follows therefore that at arbitrary value of the parameter γ the equation for R_m contains only terms of the type $m^v (d/dm)^v R_m$. Introducing the continuous variable $p = -i\nu m$, we obtain for $R(p)$ the following operator equation:

$$pR = \sum_{v=2}^{\infty} \frac{1}{v!} \varphi_v(\gamma) p^v \left(\frac{d}{dp}\right)^v R, \tag{31}$$

$$\varphi_v(\gamma) = \sum_{n=1}^{\infty} \gamma^{n-1} \frac{1}{(2\pi i)^2} \int \frac{dx\,dy}{(xy)^{n+1}} \left(\frac{x}{1-x} + \frac{y}{1-y}\right)^v. \tag{32}$$

Summing over n and integrating with respect to x, we reduce (32) to the form

$$\varphi_v(\gamma) = \frac{1}{2\pi i \gamma} \oint \frac{dy}{y} \left(\frac{\gamma}{y-\gamma} + \frac{y}{1-y}\right)^v. \tag{33}$$

The integration in (33) is along a circle of radius $\gamma < \rho < 1$ around the point $y = 0$.

We can simply transform Eq. (17) at small ν. As a result we get

$$pQ^\alpha = \sum_{v=1}^{\infty} \frac{1}{v!} \psi_v(\gamma) p^v \left(\frac{d}{dp}\right)^v Q^\alpha - i\varkappa Q^\alpha + P^\alpha, \tag{34}$$

$$\psi_v(\gamma) = \frac{1-\gamma}{2\pi i \gamma} \oint \frac{dy}{(1-y)(y-\gamma)} \left(\frac{\gamma}{y-\gamma} + \frac{y}{1-y}\right)^v. \tag{35}$$

The integration in (35) is along the same contour as in (33). The most convenient contour for (33) and (35) is the circle $\rho = \gamma^{1/2}$.

Equations (31) and (34) enable us to calculate the low-frequency asymptotic forms of the density and current correlators. From these follow, in particular, the localization of the electrons and the vanishing of the static conductivity. The first term of the exapansion σ in powers of ν then takes the form (22), and the functions $R(p)$ and $q^1(p) = Q^1(p)/i\nu$ are obtained from the solution of Eqs. (31) and (34) at $\alpha = 1$ and $\varkappa = 0$.

4. LOCALIZATION LENGTH

Equations (31) and (34) at $\alpha = 0$ enable us to find the low-frequency asymptotic form of the density correlator $X^0(\omega, k)$. Replacing in the limit of small ν the summation over m in (14) by integration with respect to p, we obtain at $\alpha = 0$:

$$X^0(\omega, k) = \frac{1}{-i\omega} \int_0^{\infty} dp\, R(p) [Q^0(p, \varkappa) + Q^0(p, -\varkappa)], \tag{36}$$

where $R(p)$ is determined by Eq. (31), and $Q^0(p, \varkappa)$ is determined by (34) with $\alpha = 0$ and $P^0(p) = R(p)$. It is seen from (36) that the density correlator $X^0(t, x)$ has as $t \to \infty$ a stationary asymptotic form $\rho(x)$:

$$\rho(x) = \lim_{t\to\infty} X^0(t, x) = \frac{1}{l} \int_{-\infty}^{\infty} \frac{d\varkappa}{2\pi} e^{i\varkappa x/l} \int_0^{\infty} dp R(p) [Q^0(p, \varkappa) + Q^0(p, -\varkappa)]. \tag{37}$$

The function $\rho(x)$ characterizes the distribution of the density of the localized electronic state.

An investigation of Eq. (34) for Q^0 enables us to determine the asymptotic form of the localized wave functions and the dependence of the localization length l_{loc} on γ. It was shown in Ref. 7 that at $\gamma \ll 1$ the form of $\rho(x)$ at large $|x| \gg l$ is determined by the position of the branch point with respect to $\varkappa$ in $Q^0(p, \varkappa)$. The position of the branch point is determined completely by the behavior of $Q^0(p, \varkappa)$ at $p \ll 1$. Indeed, Eq. (21) at large m takes the form

$$pQ^0 = p^2 \frac{d^2 Q^0}{dp^2} + 2p \frac{dQ^0}{dp} - i\varkappa Q^0 + P^0. \tag{38}$$

Substituting in the homogeneous part of this equation, at $p \ll 1$, the value $Q^0 = p^\lambda$, we get

$$\lambda(\lambda+1) - i\varkappa = 0; \quad \lambda = -1/2 \pm (1/4 + i\varkappa)^{1/2}. \tag{39}$$

We see therefore that the function $Q^0(p, \varkappa)$ has at $\gamma \ll 1$ a branch point with respect to $\varkappa$ at $\varkappa = i/4$. The position of the branch point determines completely the asymp-

totic density distribution $\rho(x)$, namely $\rho(x) \propto \exp(-|x|/4l)$ at $x \gg l$. Therefore at $\gamma \ll 1$ the localization length l_{loc} is equal to $4l$. In the general case l_{loc} is a function of γ.

In order to calculate the function $l_{loc}(\gamma)$ it is necessary to find the position of the branch point at arbitrary γ. Substituting in the homogeneous part of (34) at $p \ll 1$ the quantity $Q^0 = p^\lambda$ and making in (35) the substitution $\nu = \gamma^{1/2} e^{i\varphi}$, we obtain for λ the equation

$$f(\lambda) - 1/\gamma = i\varkappa, \tag{40}$$

$$f(\lambda) = \frac{1}{\pi\gamma}\int_0^\pi d\varphi \left(\frac{1-\gamma}{1+\gamma-2\gamma^{1/2}\cos\varphi}\right)^{1+\lambda} = \frac{1}{\gamma} P_\lambda\left(\frac{1+\gamma}{1-\gamma}\right), \tag{41}$$

where P_λ is a Legendre function. The branch point in $\varkappa$ lies at pure imaginary $\varkappa = iz$ and is obtained from the condition

$$\partial f/\partial\lambda = 0. \tag{42}$$

Its position determines the arugment of the exponential in the asymptotic form of (x):

$$\rho(x) \propto \exp(-|x|/l_{loc}), \quad |x| \gg l. \tag{43}$$

The function $l_{loc}(\gamma)$ is determined by the relation

$$l/l_{loc} = 1/\gamma - f(\lambda_0), \tag{44}$$

where λ_0 is the root of Eq. (42). It is easily seen that $f(\lambda) = f(-1-\lambda)$. Therefore Eq. (42) has a solution $\lambda_0 = -\frac{1}{2}$ in the interval $-1 < \lambda < 0$. The plot of $l_{loc}(\gamma)$ is shown in Fig. 5. It is seen from this figure that when the parameter γ changes from 0 to 1 the localization length, expressed in mean free paths l, decreases monotonically from 4 to 1. In the region $0 < \gamma < 0.25$ this decrease is still insignificant and l_{loc} can be estimated by using the results of Ref. 7.

The branch point with respect to $\varkappa$ determines not only the argument of the exponential in the asymptotic expression for $\rho(x)$, but also the pre-exponential factor. In fact, at the point $\lambda = \lambda_0$ the function $f(\lambda)$ reaches its minimum and $f''(\lambda_0) > 0$. Therefore the singularity in $\varkappa$ is a branch point of second order. Shifting the contour of integration with respect to $\varkappa$ in (37) into the upper half-plane in such a way that it follows the edges of the cut drawn from the branch point upward along the imaginary axis, and making the substitution $i\varkappa + 1/\gamma - f(\lambda_0) = -\eta^2$, we obtain at $|x| \gg l$

$$\rho(x) \approx \exp\left(\frac{-|x|}{l_{loc}}\right)\frac{1}{\pi l}\int_0^\infty \eta d\eta \exp\left(-\eta^2\frac{|x|}{l}\right)\int_0^\infty dp\, R(p)\,[Q^0(p,\eta) - Q^0(p,-\eta)]. \tag{45}$$

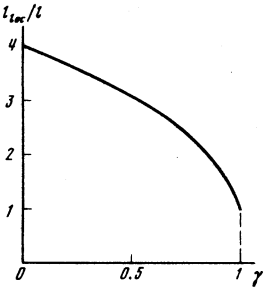

FIG. 5. Plot of the localization length *vs* γ.

At $|x| \gg l$ the integration with respect to η is over the region $\eta \ll 1$ and we can make use of the proximity of λ to λ_0. From (45) it follows that at $|x| \gg l$

$$\rho(x) \propto |x|^{-3/2}\exp(-|x|/l_{loc}). \tag{46}$$

Therefore at all γ the pre-exponential factor in the asymptotic expression for $\rho(x)$ takes the form $|x|^{-3/2}$. This statement is valid at all $0 < \gamma < 1$, but it is violated at $\gamma = 1$. The reason is that as $\gamma \to 1$ the minimum of the function in the interval $-1 < \lambda < 0$ vanishes. As a result, the character of the branch point and the pre-exponential factor in (46) change at the point $\gamma = 1$.

5. CONDUCTIVITY AND DIELECTRIC CONSTANT

Relation (22) and Eqs. (31) and (34) determine the first term of the expansion of σ in powers of ω. This term is pure imaginary and determines the value of the static dielectric constant

$$\varepsilon' = \lim_{\omega\to 0} 4\pi\sigma(\omega)/-i\omega.$$

It is easily seen that the solution of Eqs. (31) and (34) should be sought in the form of a series in powers of p. The function $R(p)$ must satisfy the boundary condition $R(0) = 1$. From the form of Eq. (31) it follows that at $p \ll 1$ the expansion of $R(p)$ in powers of p takes the form

$$R(p) = 1 + b_1 p \ln p + c_1 p + O(p^2). \tag{47}$$

Therefore in the general case $R(p)$ must be sought in the form of the series

$$R(p) = \sum_{n=0}^{\infty} (b_n \ln p + c_n) p^n; \quad b_0 = 0; \quad c_0 = 1. \tag{48}$$

Substituting (48) in (31), we obtain the following recurrence relations between b_n and c_n:

$$\beta_n b_n + (\delta_n - 1/\gamma) c_n = c_{n-1}, \tag{49}$$

$$(\delta_n - 1/\gamma) b_n = b_{n-1} \tag{50}$$

$$\delta_n = \frac{1}{\pi\gamma}\int_0^\pi d\varphi \left(\frac{1-\gamma}{1+\gamma-2\gamma^{1/2}\cos\varphi}\right)^n, \tag{51}$$

$$\beta_n = \frac{1}{\pi\gamma}\int_0^\pi d\varphi \left(\frac{1-\gamma}{1+\gamma-2\gamma^{1/2}\cos\varphi}\right)^n \ln\left(\frac{1-\gamma}{1+\gamma-2\gamma^{1/2}\cos\varphi}\right). \tag{52}$$

It is easily seen that the function $R(p)$ defined in this manner satisfies the integral equation

$$\left(p + \frac{1}{\gamma}\right)R(p) = \frac{1}{\pi\gamma}\int_0^\pi d\varphi R\left(p\frac{1-\gamma}{1+\gamma-2\gamma^{1/2}\cos\varphi}\right). \tag{53}$$

With the aid of the recurrence relations (49) and (50) we find the value s of b_n and express the coefficients c_n with $n > 1$ in terms of c_1. The value of c_1 is determined from the condition that the function $R(p)$ must decrease at infinity. In particular, at small $\gamma \ll 1$ we have $c_1 = 2C - 1$, where $C = 0.5772\ldots$ is the Euler constant. It follows from (31) that $R(p)$ decreases rapidly at large $p \gg 1$. In fact, substituting in (31) $R(p)$ with large p in the form $\exp(-\zeta(p))$ we obtain in the principal logarithmic approximation

$$\zeta(p) = 2\ln^2 p \ln\left(\frac{1+\sqrt{\gamma}}{1-\sqrt{\gamma}}\right).$$

We can show in perfect analogy that at $p \ll 1$

$$Q^1(p)=iv(a_0^1\ln^2 p+b_0^1\ln p+c_0^1+O(p)). \quad (54)$$

Introducing for convenience $q^1(p)=Q^1(p)/i\nu$, we obtain for this function a solution in series form:

$$q^1(p)=\sum_{n=0}^{\infty}(a_n^1\ln^2 p+b_n^1\ln p+c_n^1)p^n. \quad (55)$$

The coefficients a_n^1, b_n^1, and c_n^1 satisfy the recurrence relations

$$(\delta_{n+1}-1/\gamma)a_n^1=a_{n-1}^1, \quad (56)$$

$$2\beta_{n+1}a_n^1+(\delta_{n+1}-1/\gamma)b_n^1+(n+1)b_{n+1}=b_{n-1}^1, \quad (57)$$

$$\varepsilon_{n+1}a_n^1+\beta_{n+1}b_n^1+(\delta_{n+1}-1/\gamma)c_n^1+b_{n+1}+(n+1)c_n=c_{n-1}^1, \quad (58)$$

$$\varepsilon_n=\frac{1}{\pi\gamma}\int_0^{\pi}d\varphi\left(\frac{1-\gamma}{1+\gamma-2\gamma^{1/2}\cos\varphi}\right)^n\ln^2\left(\frac{1-\gamma}{1+\gamma-2\gamma^{1/2}\cos\varphi}\right). \quad (59)$$

Relations (56)–(58) are valid at $n\geq 1$. At $n=0$ the coefficients a_0^1 and b_0^1 satisfy the relations

$$2\beta_1a_0^1+b_1=0, \quad (60)$$

$$\varepsilon_1a_0^1+\beta_1b_0^1+b_1+c_1=0. \quad (61)$$

The function $q^1(p)$ satisfies the integral equation

$$\left(p+\frac{1}{\gamma}\right)q^1(p)=\frac{dR}{dp}+\frac{1}{\pi\gamma}\int_0^{\pi}\frac{d\varphi(1-\gamma)}{1+\gamma-2\gamma^{1/2}\cos\varphi}q^1\left(p\frac{1-\gamma}{1+\gamma-2\gamma^{1/2}\cos\varphi}\right). \quad (62)$$

The static dielectric constant ε' is determined by the relation

$$\varepsilon'=\varepsilon_0\int_0^{\infty}dp\frac{dR}{dp}q^1(p), \quad (63)$$

$$\varepsilon_0=16e^2l^2/v_Fs. \quad (64)$$

A plot of the $\varepsilon'(\gamma)$ calculated by numerical methods is shown in Fig. 6. It is seen from this figure that ε' decreases quite rapidly with increasing γ. The reason is the decrease of the localization length l_{loc}. When γ changes from 0 to 1 the value of $\varepsilon'/\varepsilon_0$ decreases by almost a factor of 10, from $2\zeta(3)\approx 2.42$ to 0.25.

To estimate the first term of the series in ν for Reσ, it suffices to expand Eqs. (12) and (17) to the next term in $m^{-1}\sim\nu\ll 1$. An analysis of (29) shows that the next term in m^{-1} in the equation for R_m vanishes identically, and we can use for $R(p)$ Eq. (31) as before. Expanding (17), we get

$$pQ^a+i\varkappa Q^a-P^a=\sum_{v=1}^{\infty}\frac{1}{v!}(\psi_v(\gamma)p-iv\chi_v(\gamma))p^{v-1}\left(\frac{d}{dp}\right)^vQ^a, \quad (65)$$

$$\chi_v(\gamma)=\frac{1-\gamma}{2\pi\gamma}\int_0^{\pi}\frac{d\varphi}{1+\gamma-2\gamma^{1/2}\cos\varphi}\left(\frac{2\gamma^{1/2}\cos\varphi-2\gamma}{1+\gamma-2\gamma^{1/2}\cos\varphi}\right)^v. \quad (66)$$

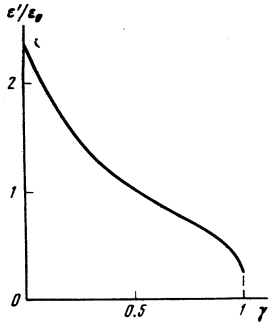

FIG. 6. Static dielectric constant *vs* γ.

It will be shown below that allowance for terms of the type $(-i\nu)p^{\nu-1}(d/dp)^\nu Q^a$ leads to logarithmic divergences in the integrals with respect to p at the lower limit, i.e., at $p\sim(-i\nu)$. These deivergences correspond to logarithmic coefficients of ν^2 in the expansion of Reσ. To calculate them it suffices to use the expansion (54) at $p\ll 1$ in the principal logarithmic approximation:

$$Q^1\approx iva_0^1\ln^2 p. \quad (67)$$

Representing $Q^1(p)$ in the form $Q^1(p)=i\nu a_0^1\ln^2 p+\nu^2Q_1^1(p)$, we get from (65)

$$Q_1^1(p)\approx a_0^1p^{-1}\ln p. \quad (68)$$

It follows from (49), (52), and (60) that

$$b_1=1/\beta_1,\ a_0^1=-1/2\beta_1^2, \quad (69)$$

$$\beta_1=-\gamma^{-1}\ln(1-\gamma). \quad (70)$$

Therefore, substituting (68) in (22), we obtain for Reσ an estimate at small:

$$\mathrm{Re}\,\sigma(\nu)\leq\sigma_0\frac{1}{6}\nu^2\left(\gamma\frac{\ln|\nu|}{\ln(1-\gamma)}\right)^3. \quad (71)$$

Expression (71) yields only an upper bound of Reσ. The reason is that the accuracy of the method used to calculate Reσ is limited by the error that arises when the summation over m in (18) is replaced by integration with respect to p. The replacement of the summation by integration leads to an error on the order of the product of the small step $-i\nu$ by the maximum of the integrand Q^1dR/dp, which is reached at $p\sim(-i\nu)$. Using the expansions (48) and (54) it can be shown that the error in the determination of Reσ is of the same order of magnitude as (71). Nevertheless, it follows from (71) that at $\nu\ll 1$

$$\mathrm{Re}\,\sigma(\nu)=\sigma_0\nu^2\Phi(\ln|\nu|)+O(\nu^3), \quad (72)$$

where Φ is a polynomial of $\ln|\nu|$, and its degree is not higher than 3. Berezinskii has shown that at $\gamma\ll 1$ we have $\Phi(\ln|\nu|)\propto\ln^2|\nu|$. Therefore the degree of Φ does not exceed two. The high-frequency expansions for Re$\sigma(\nu)$ and $\varepsilon'(\nu)$ at any γ have the usual Lorentz shape and can be easily obtained from (12) and (17) at $\nu\gg 1$:

$$\mathrm{Re}\,\sigma(\nu)\approx 8\sigma_0/\nu^2,\ \varepsilon'(\nu)\approx -4\varepsilon_0/\nu^2. \quad (73)$$

The frequency dependence of $\varepsilon'(\nu)$ and Re$\sigma(\nu)$ for arbitrary ν and γ can be obtained numerically. Indeed, because of the rapid decrease of R_m and Q_m^a at large $m\gg 1$ one can retain in the sums over m at $\nu\neq 0$ only a

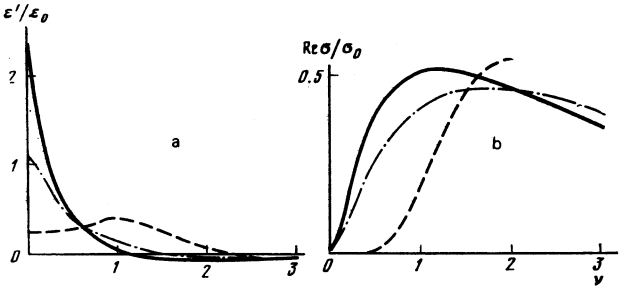

FIG. 7. Frequency dependences of ε' (ν) (a) and Reσ (ν) (b) as $\gamma\to 0$ (solid line), at $\gamma=0.5$ (dash-dot line), and at $\gamma=1$ (dashed line).

finite number $M \gg 1$ of terms. Assuming that all the R_m and Q_m^s with $m > M$ are equal to zero, we terminate the infinite system of linear equations (12) and (17), after which they can be easily solved numerically. By way of example, Figs. 7a and 7b show the plots of $\varepsilon'(\nu)$ and $\mathrm{Re}\sigma(\nu)$ at $\gamma = 0.5$. It is seen that the maximum of the conductivity remains practically unchanged in value and shifts towards larger ν. The point $\varepsilon' = 0$ in the function $\varepsilon'(\nu)$ also shifts towards larger ν. Figure 7 shows also plots of $\varepsilon'(\nu)$ and $\mathrm{Re}\sigma(\nu)$ as $\gamma \to 0$ and at $\gamma = 1$.

6. STRONG SCATTERING

The singularities connected with strong scattering of electrons by impurities manifest themselves most strongly in the case $\gamma = 1$. In this case Eqs. (12) and (17) can be solved exactly, and we can obtain explict expressions for $\varepsilon'(\nu)$ and $\mathrm{Re}\sigma(\nu)$. Physically, $\gamma = 1$ corresponds to locking of the electron between two neighboring scatters.

Retaining in (12) and (17) only the lowest terms in $1 - \gamma \ll 1$, we get

$$R_m = (1 - i\nu m)^{-1}, \tag{74}$$

$$Q_m^s(\nu, \varkappa) = P_m^s[1 - i\nu(m + {}^1/_2) + i\varkappa]^{-1}. \tag{75}$$

Substituting (74) and (75) in (18) and summing over m, we get

$$\mathrm{Re}\,\sigma(\nu) = 16\pi\sigma_0/\nu^2 \,\mathrm{sh}\,(2\pi/\nu), \tag{76}$$

$$\varepsilon'(\nu) = -\frac{4\varepsilon_0}{\nu^2}\left[1 + \frac{8}{\nu^2}\left(\beta\left(\frac{2i}{\nu}\right) + \beta\left(-\frac{2i}{\nu}\right)\right)\right], \tag{77}$$

$$\beta(x) = \frac{1}{2}\left(\psi\left(\frac{x+1}{2}\right) - \psi\left(\frac{x}{2}\right)\right), \tag{78}$$

where $\psi(x)$ is the logarithmic deviative of the Γ function. Plots of $\varepsilon'(\nu)$ and $\mathrm{Re}\sigma(\nu)$ are shown dashed in Fig. 7. We note that at small $\nu \ll 1$ we have $\mathrm{Re}\sigma(\nu) \propto \exp(-2\pi/|\nu|)$. The reason is that in the case of strong scattering by impurities the character of the low-frequency absorption changes radically. In a weak potential the electron transitions take place between spatially separated localized state so that the Mott estimate[11] $\mathrm{Re}\sigma \propto \nu^2$ is valid. In strong scattering each electron is solidly blocked between two nearest impurities, its energy spectrum becomes strictly discrete, and the low frequency absorption is due only to the expotentially unlikely fluctuation formation of very wide wells. We note that the coefficient of the ν^2 term in (71) vanishes at $\gamma \to 1$, a fact corresponding to the vanishing of the power-law absorption. A similar problem arises in the investigation of the motion of a charge-density wave in a one-dimensional random potential.[12] In this case at small $\omega\tau \ll 1$, just as in (76), we have $\mathrm{Re}\sigma(\omega) \propto \exp(-\pi/|\omega\tau|)$. The high frequency asymptotic form corresponds to absorption by almost free electrons, and $\mathrm{Re}\sigma \propto \nu^{-2}$ and $\varepsilon' \propto \nu^{-2}$. We note that the function acquires a maximum of height $0.55\ \varepsilon_0$ at $\nu \approx 0.9$. At small $\nu \ll 1$ we have

$$\varepsilon'(\nu) = \varepsilon_0({}^1/_4 + 2\nu^2 + O(\nu^4)).$$

From (74) and (75) it follows that the density correlator $X^0(\nu, \varkappa)$ has a logarithmic branch point at $\varkappa = i$. Therefore the asymptotic form of $\rho(x)$ takes at large $|x| \gg l$ the form

$$\rho(x) \propto |x|^{-1} \exp(-|x|/l).$$

7. CONCLUSION

By now, much experimental material had been accumulated on the electric and optical properties of quasi-one-dimensional conductors based on TCNQ (see the review[13]). A number of such substances were shown to have a large degree of disorder.[13] Attempts were therefore made[5,6] to interpret the experimental data on the frequency and temperature dependences of ε' and σ in TCNQ salts on the basis of localization theory. It turned out that these dependences agree well with the notion of localization of the electronic states. Agreement between theory and experiment was obtained, however, at overestimated values of the individual parameters. Thus, to reconcile simultaneously the functions $\sigma(T)$ and $\varepsilon'(T)$ in $Qn(TCNQ)_2$ and $Adz(TCNQ)_2$ it was necessary to introduce in Ref. 8 large shift $\Delta\omega_{ph}$ of the phonon frequency on account of the interaction with the electrons: $\Delta\omega_{ph} \approx 800$ K. In Ref. 5 the frequency dependences of $\varepsilon'(\omega)$ and $\sigma(\omega)$ in TTF-TCNQ (Ref. 14) was reconciled with theory at the large value $\tau^{-1} \approx 1000\ \mathrm{cm}^{-1}$.

It follows from our present results that this overestimate of the parameters is due in part to the use of the Born approximation for the impurity potential. In fact, using expression (64) and the curve of Fig. 6, we obtain for $Qn(TCNQ)_2$ at $\varepsilon' \approx 1200$, $v_F \approx 7.0 \times 10^6$ cm/sec, $c = 1/4b$, $S = 84$ Å (Ref. 8) the values $\gamma \approx 0.7$ and $l = 6b$ instead of $l = 2.5b$ ($b \approx 3.8$ Å) is the lattice constant. In $Adz(TCNQ)_2$ similarly $\gamma \approx 0.5$ and $l \approx 8b$ instead of $l \approx 4.5b$. The increased electron mean free path for scattering by impurities leads to a proportional increase of the mean free path for scattering by photons. Therefore the effective electron-phonon interaction constants, which served as the adjustment parameters in Ref. 8, decrease and $\Delta\omega_{ph} \approx 500$ K. This value is closer to the estimate $\Delta\omega_{ph} \approx 300$ K obtained from the optical data.[15]

We can analogously estimate the value of ε' in TTF-TCNQ. Comparing the frequency dependences given in Ref. 14 for $\varepsilon'(\omega)$ and $\mathrm{Re}\sigma(\omega)$ with the plots in Fig. 7 at $\gamma = 0.5$ we obtain $\tau^{-1} \approx 600\ \mathrm{cm}^{-1}$ in place of $1000\ \mathrm{cm}^{-1}$. This yields a mean free path on the order of ten lattice constants and agrees better with the estimates of the degree of disorder in TTF-TCNQ. Thus, allowance for the strong interaction of the electrons with the impurities leads to more reasonable values of the fit parameters.

The problem of calculating the frequency dependences of ε' and $\mathrm{Re}\sigma$ in the case of weak disorder was solved by using numerical simulation in Ref. 16. The curves given in Ref. 16 are close to our present results at small γ. The distribution of the electron density and the localization length were investigated by a similar method in Refs. 17 and 18. Some difference between the values of l_{loc} are due to the fact that this value was determined in Refs. 17 and 18 from the asymptotic value of the averaged wave function $\psi(x)$, which decreases more rapidly because of the averaging of the phase.

In conclusion, the author is greatful to V. L. Berezinskii, V. I. Mel'nikov, and É. I. Rashba for a useful discussion of the results of the work.

[1]N. F. Mott and W. D. Twose, Adv. Phys. **10**, 107 (1961).
[2]B. I. Halperin, Adv. Chem. Phys. **13**, 123 (1967); Yu. A. Bychkov, Zh. Eksp. Teor. Fiz. **65**, 427 (1973) [Sov. Phys. JETP **38**, 209 (1974)]; C. T. Papatrantafillou, Phys. Rev. B **7**, 5386 (1972).
[3]V. L. Berezinskiĭ, Zh. Eksp. Teor. Fiz. **65**, 1251 (1973) [Sov. Phys. JETP **38**, 620 (1974)].
[4]A. A. Goglin, Zh. Eksp. Teor. Fiz. **71**, 1912 (1976) [Sov. Phys. JETP **44**, 1003 (1976)].
[5]A. A. Gogolin and V. I. Mel'nikov, Phys. Status Solidi B **88**, 377 (1978).
[6]A. A. Abrikosov and I. A. Ryzhkin, Zh. Eksp. Teor. Fiz. **71**, 1916 (1976) [Sov. Phys. JETP **44**, 1005 (1976)].
[7]A. A. Gogolin, V. I. Mil'nikov, and É. I. Rashba, Zh. Eksp. Teor. Fiz. **69**, 327 (1975) [Sov. Phys. JETP **42**, 168 (1975)].
[8]A. A. Gogolin, S. P. Zolotukhin, V. I. Mel'nikov, E. I. Rashba, and I. F. Shchegolev, Pis'ma Zh. Eksp. Teor. Fiz. **22**, 564 (1975) [JETP Lett. **22** 278 (1975)].
[9]A. A. Abrikosov, L. P. Gor'kov, and I. E. Dzyaloshinskiĭ, Metody kvantovoĭ teorii polya v statisticheskoĭ fizike (Quantum Field Theoretical Methods in Statistical Physics), Fizmatgiz, 1962 [Pergamon, 1965]
[10]L. D. Landau and E. M. Lifshitz, Kvantovaya mekhnaika (Quantum Mechanics), Nauka, 1974 [Pergamon].
[11]N. F. Mott, Adv. Phys. **18**, 49 (1967) [Russian translation].
[12]L. P. Gor'kov, Pis'ma Zh. Eksp. Teor. Fiz. **25**, 384 (1977) [JETP Lett. **25**, 358 (1977)].
[13]I. F. Shchegolev, Phys. Status Solidi A **12**, 9 (1972).
[14]D. B. Tanner, C. S.Jacobsen, A. F. Garito, and A. J. Heeger, Phys. Rev. B **13**, 3381 (1976).
[15]M. G.Kaplunov, T. P. Panova, E. B.Yagubskiĭ, and Yu. G. Borod'ko, Zh. Strukt. Khim. **13**, 440 (1972).
[16]R. L. Bush, Phys. Rev. B **13**, 805 (1976).
[17]R. L. Bush, Phys. Rev. B **6**, 1182 (1972).
[18]C. T. Papatriantafillou and E. N. Econonou, Phys. Rev. B **13**, 805 (1976).

Translated by J. G. Adashko

Stimulation of superconductivity in an inhomogeneous bridge in a microwave field

L. G. Aslamazov

Moscow Institute of Steel and Alloys
(Submitted 15 November 1978)
Zh. Eksp. Teor. Fiz. **76**, 1775–1780 (May 1979)

Stimulation of superconductivity in a bridge whose neck has a lower critical temperature than the shores is investigated. It is shown that, depending on the microwave-field frequency, the relative contributions made to the stimulation by the "trembling" of the potential well and by the electric field vary, and this leads to different types of phase diagrams of the bridge.

PACS numbers: 85.25. + k, 74.10. + v

Irradiation of a superconductor by a microwave field changes the electron energy distribution, and this disequilibrium can cause a substantial increase of the critical parameters of the superconductor.[1] In superconductors with constrictions (bridges, point contacts, etc.) the electron energy diffusion is caused both by direct acceleration by the electric field,[1,2] and by the "trembling" of the potential well produced as a result of the lowering of the value of the order parameter in the constriction region.[3] The energy of the electrons trapped in the constriction region increases upon reflection from the walls of the trembling well, and the magnitude of the effect depends substantially on the character of the dependence of the order parameter on the coordinates.

For a homogeneous superconductor, the decrease of the order parameter Δ in the constriction region is due to the increase of the density of the superconducting current. At the critical value of the current, Δ has a power-law dependence on the coordinates, and the trembling of the well leads to a substantial increase of the critical current of the bridge in the microwave field.

This paper deals with an inhomogeneous bridge in which the neck has a critical temperature T_c somewhat lower than the critical temperature T_{c0} of the shores of the bridge. The dependence of the order parameter on the coordinates is exponential. In such a bridge the effects of stimulation can lead to a preservation of the superconductivity up to temperatures close to T_{c0}.

1. SUPERCONDUCTIVITY STIMULATION DUE TO THE TREMBLING OF THE POTENTIAL WELL

The change of the electron distribution function in the microwave field depends on the irradiation power. At sufficiently high irradiation powers an equipartition is established of the energies of the electrons trapped in the region of the contact:

$$f(\varepsilon)=\Delta_0/2T, \quad \varepsilon<\Delta_0, \tag{1}$$

where Δ_0 are the values of the order parameter at the shores of the bridge.[3] The electrons with energies $E>\Delta_0$, for bridges that are not too long, can diffuse freely from the contact and therefore have an equilibrium energy distribution (the microwave current density in the shores is negligibly small). As a result, the nonequilibrium term in the Ginzburg-Landau equation for the order parameter[3] takes in the limit of high irradiation power the form

$$\Phi(\Delta)=\Delta\int_{\Delta}^{\infty}\left(f-\operatorname{th}\frac{\varepsilon}{2T}\right)\frac{d\varepsilon}{(\varepsilon^2-\Delta^2)^{1/2}}=\frac{\Delta\Delta_0}{2T}\left[\ln\frac{1+(1-\Delta^2/\Delta_0^2)^{1/2}}{\Delta/\Delta_0}-\left(1-\frac{\Delta^2}{\Delta_0^2}\right)^{1/2}\right]. \tag{2}$$

The superconducting transition temperature T_c^P of the

 0038-5646/79/050902-04$02.40